Input-to-State Stable Bilateral Teleoperation by Dynamic Interconnection and Damping Injection: Theory and Experiments

Article *in* IEEE Transactions on Industrial Electronics · April 2019

DOI: 10.1109/TIE.2019.2907448

3 authors:


Yuan Yang
Polytechnique Montréal


Daniela Constantinescu
University of Victoria


Yang Shi
University of Victoria

Input-to-State Stable Bilateral Teleoperation by Dynamic Interconnection and Damping Injection: Theory and Experiments

Yuan Yang, Daniela Constantinescu, *Member, IEEE* and Yang Shi, *Fellow, IEEE*

***Abstract*—In bilateral teleoperation, the human operating the master and the environment interacting with the slave are part of the force feedback loop. Yet, both have time-varying and unpredictable dynamics and are challenging to model. Conventional sidestepping of the demand for their models in the stability analysis assumes passive user and environment, and controls the master-communications-slave system to be passive too. This paper circumvents the need for user and environment models in a novel way: it regards their forces as external excitations for a semi-autonomous feedback loop, which it outfits with a dynamic interconnection and damping injection controller that renders time-delay teleoperation exponentially input-to-state stable. The controller uses the position and velocity of the local robot and the delayed position transmitted from the other side to robustly synchronize the master and slave under the user and environment perturbations. Lyapunov-Krasovskii stability analysis shows that the strategy (i) can confine the position error between the master and slave to an invariant set, and (ii) can drive it exponentially to a globally attractive set. The approach has practical relevance for telemanipulation tasks with given precision requirements. Experiments with a pair of Geomagic Touch robots validate the strategy compared to state-of-the-art robust position tracking designs.**

***Index Terms*—telerobotics, nonlinear systems, lyapunov methods**

I. INTRODUCTION

As a tool for remote sensing and manipulation, a bilateral teleoperator strives to synchronize its master and slave robots tightly, and to provide its human operator with useful haptic cues about the slave-environment interactions. Therefore, the bilateral teleoperation feedback loop includes the human who operates the master, the environment which interacts with the slave and the master-communications-slave system [1]. Because operators vary their dynamics according to their volition, and environments are typically unknown, neither are predictable or trivial to model [2]. Additionally, the master and slave exchange information distorted by time-varying communication delays [3]. Thus, bilateral teleoperation is a nonlinear, time-varying and interconnected system with communication delays and uncertain user and environment dynamics [4].

Manuscript received October 2, 2018; revised December 27, 2018 and February 17, 2019; accepted March 1, 2019.

The authors are with the Department of Mechanical Engineering, University of Victoria, Victoria, BC V8W 2Y2 Canada (e-mail: yangyuan@uvic.ca; danielac@uvic.ca; yshi@uvic.ca).

The physical interaction between the robotic master-communications-slave system (aka the teleoperator) and the user and the environment (aka its external terminators) involve exchange of energy [5]. As a key theory for modeling and controlling the exchange of energy among interconnected systems, passivity is often pivotal to the rigorous treatment of closed-loop teleoperation without user and environment models [6]. Existing research exploits the stability of the feedback interconnection of passive systems by assuming passive operator and environment and by employing Lyapunov-like analysis [7] or energy monitoring [8] to offer controllers which maintain teleoperators with time delays passive.

Scattering-based, damping injection and adaptive strategies can all be designed to provably stabilize bilateral teleoperation with a unified Lyapunov-like energy function. Scattering or wave-based control can render the time-delay communication channel passive, as well as reduce wave reflections [9] and improve trajectory tracking [10], [11] and transparency [11]–[15]. Damping injection control, Proportional-Derivative plus damping (PD+d) [16] or Proportional plus damping (P+d) [17], and extensions to position-force architectures [18], output feedback [19] and bounded actuation [20] implement a virtual spring between, and local dampers at, the master and slave sites. Joint-space [21], [22] and task-space [23], [24] adaptive strategies can synchronize master and slave robots with uncertain parameters and constant delays.

Energy monitoring-based control can render the teleoperator passive by dynamic damping injection, dynamic modulation of the nominal control force, or both. Time-domain passivity control [25], [26] and extensions to eliminate position drift [27] inject sufficient damping to dissipate the delay-induced energy at each step. The energy bounding [28] and passive set-position modulation (PSPM) [29] strategies regulate the nominal control inputs to ensure that the teleoperator generates less energy than its physical and control damping dissipates. The two-layer approach [8], [30] modulates the forces computed in the transparency layer and adds damping in the passivity layer to limit energy accumulation in the system.

Input-output stability provides another path to rigorous stability of time-delay systems with uncertain dynamics [31]. In particular, input-to-state stability has diminished the conservatism of passive strategies in haptic rendering [32], and has offered robust position tracking for time-delay bilateral shared control of an aerial vehicle [33].

This paper introduces a novel strategy for input-to-state stable (ISS) time-delay bilateral teleoperation. The new strategy combines a dynamic master-slave interconnection with dynamic damping injections to each robot. Although force-reflection [8], [30], [34], [35] and force-reproduction [36]–[39] architectures can improve transparency, force and acceleration measurements are unavailable or noisy for many commercial robots. Therefore, the proposed strategy relies on a position-position structure. Its controllers require only the position and velocity of the local robot, plus the delayed position of the remote robot. Compared to conventional controllers based on Lyapunov-like analysis [7] or energy-monitoring [8], which stably connect the master and slave but cannot quantify their error a-priori, the proposed strategy can limit the impact of the user and environment on it. A key design step to bring about this property is the transformation of the system dynamics into a first-order passive form through properly designed sliding surfaces. Compared to conventional feedback passivation [40], the proposed strategy suppresses the Coriolis and centrifugal effects of the Euler-Lagrange dynamics without compensation, by simply modulating the Proportional and damping gains according to the local velocities. To the authors' best knowledge, the dynamic interconnections and damping injection strategy in this paper is the first to make time-delay teleoperation exponentially ISS based on Proportional plus damping control.

The P+d [17], PSPM [29] and two-layer [8], [41] approaches are most closely related to the dynamic strategy introduced in this paper. Whereas the P+d and PSPM algorithms synchronize the master and slave exactly in the absence of user and environment forces but over-inject constant damping compared to the two-layer method, the dynamic strategy in this paper offers a unique property for robust position tracking in time-delay bilateral teleoperation: given full (unlimited) actuation, it can confine the master-slave position error to a prescribed invariant set, and can drive it exponentially to a globally attractive set which includes the origin. The invariant set quantifies the maximum master-slave position error during teleoperation. The globally attractive set measures their position error at steady-state. The rate of exponential convergence from the invariant set to the attractive set quantifies the transient response of the teleoperator. More importantly, Lyapunov stability analysis shows that upper bounds on the Lebesgue measures of the invariant and globally attractive sets, and the rate of convergence to the latter, depend on the control gains. This unique property of the proposed dynamic interconnection and damping injection strategy can benefit precision telemanipulation tasks: because constraints on the master-slave position error map to a feasible set for the ISS bilateral teleoperation, proper selection of the control gains can make the feasible set positively invariant. Thus, the control gains of the proposed strategy can be selected to tighten the master-slave coupling, and to indirectly convey the slave-environment interactions to the operator [30]. Experiments with a pair of Geomagic Touch haptic robots compare the controller proposed in this paper to state-of-the-art controllers.

II. Preliminaries

A. System Dynamics

Let the master and slave robots be n-degree-of-freedom (n-DOF) serial manipulators with revolute joints. Their joint-space dynamics are:

$$\begin{aligned}\mathbf{M}_m(\mathbf{q}_m)\cdot\ddot{\mathbf{q}}_m+\mathbf{C}_m(\mathbf{q}_m,\dot{\mathbf{q}}_m)\cdot\dot{\mathbf{q}}_m=&\boldsymbol{\tau}_m+\boldsymbol{\tau}_h,\\ \mathbf{M}_s(\mathbf{q}_s)\cdot\ddot{\mathbf{q}}_s+\mathbf{C}_s(\mathbf{q}_s,\dot{\mathbf{q}}_s)\cdot\dot{\mathbf{q}}_s=&\boldsymbol{\tau}_s+\boldsymbol{\tau}_e,\end{aligned}\tag{1}$$

where the subscript $i = m, s$ indexes master and slave quantities, $\ddot{\mathbf{q}}_i$, $\dot{\mathbf{q}}_i$ and $\mathbf{q}_i$ are joint acceleration, velocity and position, $\mathbf{M}_i(\mathbf{q}_i)$ and $\mathbf{C}_i(\mathbf{q}_i, \dot{\mathbf{q}}_i)$ are matrices of inertia and of Coriolis and centrifugal effects, $\boldsymbol{\tau}_i$ are control torques, and $\boldsymbol{\tau}_h$ and $\boldsymbol{\tau}_e$ are user and environment torques.

The following properties of the dynamics (1), and assumptions on communication delays and on user and environment torques, facilitate later control design and stability analysis.

- P.1 The inertia matrix $\mathbf{M}_i(\mathbf{q}_i)$ is symmetric, positive definite and uniformly bounded by $\mathbf{0}\prec\lambda_{i1}\mathbf{I}\preceq\mathbf{M}_i(\mathbf{q}_i)\preceq\lambda_{i2}\mathbf{I}\prec\infty$, with λ_{i1} and λ_{i2} positive constants.
- P.2 The matrix $\dot{\mathbf{M}}_i(\mathbf{q}_i)-2\mathbf{C}_i(\mathbf{q}_i,\dot{\mathbf{q}}_i)$ is skew-symmetric.
- P.3 There exists $c_i > 0$ such that $\|\mathbf{C}_i(\mathbf{q}_i,\mathbf{x})\cdot\mathbf{y}\|\leq c_i\cdot\|\mathbf{x}\|\cdot\|\mathbf{y}\|, \forall\mathbf{q}_i,\mathbf{x},\mathbf{y}$.
- A.1 The time-varying communication delays from robot i to robot j, d_i, are bounded, $0\leq d_i\leq\overline{d}_i$, for $i, j = m, s$.
- A.2 The joint torques due to operator $\boldsymbol{\tau}_h$ and environment $\boldsymbol{\tau}_e$ forces are bounded by $\|\boldsymbol{\tau}_k\|\leq\overline{\tau}_k$, $k = h, e$.

In these properties and assumptions, as in the remainder of the paper, $\|\mathbf{v}\|=\sqrt{\mathbf{v}^{\mathsf{T}}\mathbf{v}}$ is the Euclidean norm of vector $\mathbf{v}$.

B. Input-to-State Stability

This section overviews the definitions and theorems required by the stability analysis in Section III.

A function $\alpha:\mathbb{R}_{\geq0}\mapsto\mathbb{R}_{\geq0}$ is of class $\mathcal{K}$ if it is continuous, strictly increasing and $\alpha(0) = 0$; of class $\mathcal{K}_\infty$ if it is of class $\mathcal{K}$ and unbounded; of class $\mathcal{L}$ if it decreases to zero as its argument tends to $+\infty$. A function $\beta:\mathbb{R}_{\geq0}\times\mathbb{R}_{\geq0}\mapsto\mathbb{R}_{\geq0}$ is of class $\mathcal{KL}$ if it is of class $\mathcal{K}$ in its first argument and of class $\mathcal{L}$ in the second argument. Let $\mathcal{C}([-r,0];\mathbb{R}^m)$ denote the set of the continuous functions defined on $[-r, 0]$ and with values in $\mathbb{R}^m$. For any essentially bounded function $\boldsymbol{\phi}\in\mathcal{C}([-r,0];\mathbb{R}^m)$, let $|\boldsymbol{\phi}|_r=\sup_{-r\leq\tau\leq0}\|\boldsymbol{\phi}(\tau)\|$ and $|\boldsymbol{\phi}|_a$ be a norm of $\boldsymbol{\phi}$ such that:

$$\gamma_a\cdot\|\boldsymbol{\phi}(0)\|\leq|\boldsymbol{\phi}|_a\leq\overline{\gamma}_a\cdot|\boldsymbol{\phi}|_r\tag{2}$$

for some positive reals γ_a and $\overline{\gamma}_a$.

D.1 [42] The nonlinear delay-free system

$$\dot{\mathbf{x}}(t)=f(\mathbf{x}(t),\mathbf{u}(t))\tag{3}$$

is ISS with input $\mathbf{u}(t)\in\mathbb{R}^l$ and state $\mathbf{x}(t)\in\mathbb{R}^m$ if there exist functions $\alpha\in\mathcal{K}$ and $\beta\in\mathcal{KL}$ such that:

$$\|\mathbf{x}(t)\|\leq\beta\left(\|\mathbf{x}(0)\|,t\right)+\alpha\left(\sup_{0\leq\tau\leq t}\|\mathbf{u}(\tau)\|\right),\ \forall t\geq0.\tag{4}$$

D.2 [43] The nonlinear time-delay system:

$$\begin{aligned}\dot{\mathbf{x}}(t)=&f(\mathbf{x}_t,\mathbf{u}(t)),\quad t\geq0\ a.e.,\\ \mathbf{x}(\tau)=&\boldsymbol{\xi}_0(\tau),\quad\tau\in[-r,0],\end{aligned}\tag{5}$$

with $\mathbf{x}_t : [-r, 0] \mapsto \mathbb{R}^m$ the standard function $\mathbf{x}_t(\tau) = \mathbf{x}(t+\tau)$, and r the maximum involved delay, $f : \mathcal{C}([-r,0];\mathbb{R}^m) \times \mathbb{R}^l \mapsto \mathbb{R}^m$, and $\boldsymbol{\xi}_0 \in \mathcal{C}([-r,0];\mathbb{R}^m)$, is ISS with input $\mathbf{u}(t) \in \mathbb{R}^l$ and state $\mathbf{x}(t) \in \mathbb{R}^m$ if there exist functions $\alpha \in \mathcal{K}$ and $\beta \in \mathcal{KL}$ such that:

$$\|\mathbf{x}(t)\| \leq \beta\left(|\boldsymbol{\xi}_0|_r, t\right) + \alpha\left(\sup_{0\leq\tau\leq t} \|\mathbf{u}(\tau)\|\right), \forall t \geq 0. \quad (6)$$

Because the time-delay system (5) is infinite dimensional [31], the input-to-state stability of it is defined differently than that of the delay-free system (3). Correspondingly, the following two theorems using ISS-Lyapunov functions and Lyapunov-Krasovskii functionals facilitate proving ISS teleoperation without delays and with time-varying delays, respectively.

T.1 [42] The delay-free system (3) is ISS if and only if there exist an ISS-Lyapunov function $V : \mathbb{R}^m \mapsto \mathbb{R}_{\geq 0}$, and functions $\alpha_1, \alpha_2 \in \mathcal{K}_\infty$, $\alpha_3, \rho \in \mathcal{K}$ such that:
  a) $\alpha_1(\|\mathbf{x}\|) \leq V(\mathbf{x}) \leq \alpha_2(\|\mathbf{x}\|)$, $\forall \mathbf{x} \in \mathbb{R}^m$;
  b) $\dot{V}(\mathbf{x}, \mathbf{u}) \leq -\alpha_3(\|\mathbf{x}\|)$, $\forall \mathbf{x} \in \mathbb{R}^m, \mathbf{u} \in \mathbb{R}^l : \|\mathbf{x}\| \geq \rho(\|\mathbf{u}\|)$.

T.2 [43] The time-delay system (5) is ISS if there is a Lyapunov-Krasovskii functional $V : \mathcal{C}([-r,0];\mathbb{R}^m) \mapsto \mathbb{R}_{\geq 0}$, functions $\alpha_1, \alpha_2 \in \mathcal{K}_\infty$, $\alpha_3, \rho \in \mathcal{K}$ such that:
  a) $\alpha_1(\|\mathbf{x}\|) \leq V(\mathbf{x}_t) \leq \alpha_2(|\mathbf{x}_t|_a)$, $\forall \mathbf{x}_t \in \mathcal{C}([-r,0];\mathbb{R}^m)$;
  b) $\dot{V}(\mathbf{x}_t, \mathbf{u}) \leq -\alpha_3(|\mathbf{x}_t|_a)$, $\forall \mathbf{x}_t \in \mathcal{C}([-r,0];\mathbb{R}^m), \mathbf{u} \in \mathbb{R}^l : |\mathbf{x}_t|_a \geq \rho(\|\mathbf{u}\|)$.

III. Main Result

This section presents the control design and stability analysis for ISS bilateral teleoperation, considering communications both without, and with time-varying, delays.

A. ISS Teleoperation Without Time Delays

Define sliding surfaces for the master and slave robots by:

$$\mathbf{s}_i = \dot{\mathbf{q}}_i + \sigma \cdot (\mathbf{q}_i - \mathbf{q}_j), \quad (7)$$

where $i, j = m, s$ and $i \neq j$, and $\sigma > 0$ is a constant to be determined. Then, the dynamics (1) can be transformed to:

$$\mathbf{M}_i(\mathbf{q}_i) \cdot \dot{\mathbf{s}}_i + \mathbf{C}_i(\mathbf{q}_i, \dot{\mathbf{q}}_i) \cdot \mathbf{s}_i = \boldsymbol{\tau}_i + \boldsymbol{\tau}_k + \sigma \cdot \boldsymbol{\Delta}_i, \quad (8)$$

where $i = m, s$ and $k = h, e$, respectively, and the state-dependent master and slave mismatches are:

$$\boldsymbol{\Delta}_i = \mathbf{M}_i(\mathbf{q}_i) \cdot (\dot{\mathbf{q}}_i - \dot{\mathbf{q}}_j) + \mathbf{C}_i(\mathbf{q}_i, \dot{\mathbf{q}}_i) \cdot (\mathbf{q}_i - \mathbf{q}_j), \quad (9)$$

with $i, j = m, s$ and $i \neq j$.

The master and slave receive each other's position instantly, and their dynamic interconnection and damping injection controllers are:

$$\boldsymbol{\tau}_i = -\mathbf{K}_i(\dot{\mathbf{q}}_i) \cdot \mathbf{s}_i - \mathbf{P} \cdot (\mathbf{q}_i - \mathbf{q}_j) - \mathbf{D}_i \dot{\mathbf{q}}_i, \quad (10)$$

where $i, j = m, s$ and $i \neq j$, and $\mathbf{K}_i(\dot{\mathbf{q}}_i)$, $\mathbf{P}$ and $\mathbf{D}_i$ are diagonal positive definite gain matrices to be designed.

Remark 1. The velocity-dependent gains $\mathbf{K}_i(\dot{\mathbf{q}}_i)$ are designed to suppress the state-dependent mismatch $\boldsymbol{\Delta}_i$ in (9). Rewriting (10) in the form:

$$\boldsymbol{\tau}_i = -\Big[\mathbf{P} + \sigma \cdot \mathbf{K}_i(\dot{\mathbf{q}}_i)\Big] \cdot (\mathbf{q}_i - \mathbf{q}_j) - \Big[\mathbf{D}_i + \mathbf{K}_i(\dot{\mathbf{q}}_i)\Big] \cdot \dot{\mathbf{q}}_i,$$

where $i, j = m, s$ and $i \neq j$, reveals that the controller dynamically modulates the master-slave interconnection and the local damping through $\mathbf{K}_i(\dot{\mathbf{q}}_i)$. The transformed system dynamics (8) are input-output passive with input $\boldsymbol{\tau}_i + \boldsymbol{\tau}_k + \sigma \cdot \boldsymbol{\Delta}_i$ and output $\mathbf{s}_i$, where $i = m, s$ and $k = h, e$, respectively. However, the teleoperator (1) in closed-loop with the controller (10) is not guaranteed stable because the modulated interconnection, shown as a yellow shaded area in Figure 1, may not be passive [29] and thus may render the teleoperator non-passive. The following rigorous analysis is required to show ISS teleoperation.

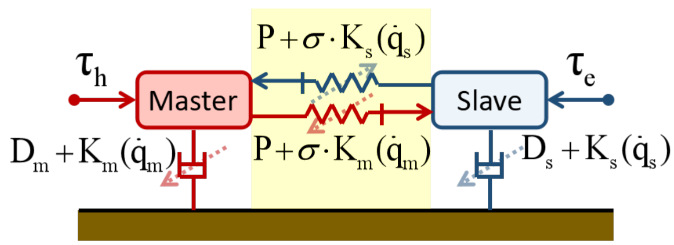

Figure 1. The teleoperator (1) in closed-loop with the control (10).

The following Lyapunov candidate:

$$V = \frac{1}{2} \sum_{i=m,s} \mathbf{s}_i^\mathsf{T} \mathbf{M}_i(\mathbf{q}_i) \cdot \mathbf{s}_i + \frac{1}{2} \cdot (\mathbf{q}_m - \mathbf{q}_s)^\mathsf{T} \mathbf{P} \cdot (\mathbf{q}_m - \mathbf{q}_s), \quad (11)$$

serves to evaluate stability. After using property P.2, the time derivative of V along the closed-loop dynamics (8) with the control (10) can be evaluated as:

$$\begin{aligned} \dot{V} = & \sum_{i=m,s} \left[\sigma \cdot \mathbf{s}_i^\mathsf{T} \boldsymbol{\Delta}_i - \mathbf{s}_i^\mathsf{T} \mathbf{K}_i(\dot{\mathbf{q}}_i) \cdot \mathbf{s}_i - \mathbf{s}_i^\mathsf{T} \mathbf{D}_i \dot{\mathbf{q}}_i\right] \\ & + \mathbf{s}_m^\mathsf{T} \boldsymbol{\tau}_h + \dot{\mathbf{q}}_m^\mathsf{T} \mathbf{P} \cdot (\mathbf{q}_m - \mathbf{q}_s) - \mathbf{s}_m^\mathsf{T} \mathbf{P} \cdot (\mathbf{q}_m - \mathbf{q}_s) \\ & + \mathbf{s}_s^\mathsf{T} \boldsymbol{\tau}_e + \dot{\mathbf{q}}_s^\mathsf{T} \mathbf{P} \cdot (\mathbf{q}_s - \mathbf{q}_m) - \mathbf{s}_s^\mathsf{T} \mathbf{P} \cdot (\mathbf{q}_s - \mathbf{q}_m). \end{aligned} \quad (12)$$

The definitions of $\boldsymbol{\Delta}_i$ in (9) together with properties P.1 and P.3 lead to the following inequalities for $i = m, s$:

$$\begin{aligned} \mathbf{s}_i^\mathsf{T} \boldsymbol{\Delta}_i \leq & \lambda_{i2} \cdot \left(\mathbf{s}_i^\mathsf{T} \mathbf{s}_i + \frac{1}{2} \dot{\mathbf{q}}_m^\mathsf{T} \dot{\mathbf{q}}_m + \frac{1}{2} \dot{\mathbf{q}}_s^\mathsf{T} \dot{\mathbf{q}}_s\right) \\ & + c_i \cdot \left(\|\dot{\mathbf{q}}_i\|^2 \cdot \mathbf{s}_i^\mathsf{T} \mathbf{s}_i + \frac{\|\mathbf{q}_m - \mathbf{q}_s\|^2}{4}\right). \end{aligned} \quad (13)$$

Remark 2. The inequalities (13) show that the impact of master and slave mismatches can be upper-bounded using the velocities of the two robots and their position error. Thus, they indicate the demand for a dynamic interconnection and damping injection strategy. More specifically, as will be illustrated in Equations (16)-(17), the terms $\|\dot{\mathbf{q}}_i\|^2 \cdot \mathbf{s}_i^\mathsf{T} \mathbf{s}_i$ in inequalities (13) can be dominated by selecting velocity-dependent gains $\mathbf{K}_i(\dot{\mathbf{q}}_i)$ in the controls $\boldsymbol{\tau}_i$. Alternatively, the terms $\mathbf{s}_i^\mathsf{T} \mathbf{C}_i(\mathbf{q}_i, \dot{\mathbf{q}}_i) \cdot (\mathbf{q}_m - \mathbf{q}_s)$ can be bounded by $c_i \cdot \left(\|\mathbf{q}_m - \mathbf{q}_s\|^2 \cdot \mathbf{s}_i^\mathsf{T} \mathbf{s}_i + \frac{1}{4} \cdot \dot{\mathbf{q}}_i^\mathsf{T} \dot{\mathbf{q}}_i\right)$, and the gains $\mathbf{K}_i$ can be updated based on the master-slave position error. Therefore, both the master and slave velocities and their position error can be used to dynamically modulate their coupling and local damping injection, to achieve ISS bilateral teleoperation.

The definitions of the sliding surfaces $\mathbf{s}_i$ lead to:

$$\begin{aligned} &- \mathbf{s}_i^\mathsf{T}\mathbf{P}\cdot(\mathbf{q}_i-\mathbf{q}_j) - \mathbf{s}_i^\mathsf{T}\mathbf{D}_i\dot{\mathbf{q}}_i + \dot{\mathbf{q}}_i^\mathsf{T}\mathbf{P}\cdot(\mathbf{q}_i-\mathbf{q}_j) \\ \le &-\sigma\cdot(\mathbf{q}_i-\mathbf{q}_j)^\mathsf{T}\left(\mathbf{P}-\frac{\mu_i}{4}\cdot\mathbf{D}_i\right)\cdot(\mathbf{q}_i-\mathbf{q}_j) \\ &-\left(1-\frac{\sigma}{\mu_i}\right)\cdot\dot{\mathbf{q}}_i^\mathsf{T}\mathbf{D}_i\dot{\mathbf{q}}_i, \end{aligned} \tag{14}$$

where $i,j=m,s$, $i\neq j$ and $\mu_i>0$. Further algebraic manipulations yield:

$$\mathbf{s}_m^\mathsf{T}\boldsymbol{\tau}_h+\mathbf{s}_s^\mathsf{T}\boldsymbol{\tau}_e \le \sum_{i=m,s}\omega_i\cdot\mathbf{s}_i^\mathsf{T}\mathbf{s}_i+\frac{1}{4}\cdot\left(\frac{\|\boldsymbol{\tau}_h\|^2}{\omega_m}+\frac{\|\boldsymbol{\tau}_e\|^2}{\omega_s}\right), \tag{15}$$

where $\omega_i>0$, $i=m,s$.

After substitutions from Equations (13)-(15), the derivative of the Lyapunov candidate (12) can then be bounded by:

$$\begin{aligned} \dot{V}\le &-\sum_{i=m,s}\left(\mathbf{s}_i^\mathsf{T}\overline{\mathbf{K}}_i(\dot{\mathbf{q}}_i)\cdot\mathbf{s}_i+\dot{\mathbf{q}}_i^\mathsf{T}\overline{\mathbf{D}}_i\dot{\mathbf{q}}_i\right) \\ &-(\mathbf{q}_m-\mathbf{q}_s)^\mathsf{T}\overline{\mathbf{P}}\cdot(\mathbf{q}_m-\mathbf{q}_s)+\frac{\|\boldsymbol{\tau}_h\|^2+\|\boldsymbol{\tau}_e\|^2}{4\omega}, \end{aligned} \tag{16}$$

where $\omega=\min(\omega_m,\omega_s)$ and:

$$\begin{aligned} \overline{\mathbf{K}}_i(\dot{\mathbf{q}}_i)=&\mathbf{K}_i(\dot{\mathbf{q}}_i)-\left(\omega_i+\sigma\cdot\lambda_{i2}+\sigma\cdot c_i\cdot\|\dot{\mathbf{q}}_i\|^2\right)\cdot\mathbf{I}, \\ \overline{\mathbf{D}}_i=&\left(1-\frac{\sigma}{\mu_i}\right)\cdot\mathbf{D}_i-\frac{\sigma}{2}\cdot\left(\lambda_{m2}+\lambda_{s2}\right)\cdot\mathbf{I}, \\ \overline{\mathbf{P}}=&2\sigma\cdot\mathbf{P}-\frac{\sigma}{4}\cdot\sum_{i=m,s}\left(\mu_i\cdot\mathbf{D}_i+c_i\cdot\mathbf{I}\right). \end{aligned} \tag{17}$$

Theorem 1. *The teleoperator* (1) *with the control* (10) *is ISS with input* $\mathbf{u}=[\boldsymbol{\tau}_h^\mathsf{T}\ \boldsymbol{\tau}_e^\mathsf{T}]^\mathsf{T}$ *and state* $\mathbf{x}=[\dot{\mathbf{q}}_m^\mathsf{T}\ \dot{\mathbf{q}}_s^\mathsf{T}\ (\mathbf{q}_m-\mathbf{q}_s)^\mathsf{T}]^\mathsf{T}$ *if the control gains* $\mathbf{K}_i(\dot{\mathbf{q}}_i)$, $\mathbf{D}_i$, $\mathbf{P}$, σ *and positive parameters* μ_i, ω_i, κ, $i=m,s$, *satisfy:*

$$\overline{\mathbf{P}}\succeq\frac{\kappa}{2}\cdot\mathbf{P},\quad \overline{\mathbf{K}}_i(\dot{\mathbf{q}}_i)\succeq\frac{\kappa}{2}\cdot\lambda_{i2}\cdot\mathbf{I}\quad \textit{and}\quad \overline{\mathbf{D}}_i\succeq\mathbf{0}. \tag{18}$$

Proof. The Property P.1 and Equations (11) and (7) together lead to:

$$V\ge\sum_{i=m,s}\frac{\lambda_{i1}}{2}\cdot\|\mathbf{s}_i\|^2+\frac{p}{2}\cdot\|\mathbf{q}_m-\mathbf{q}_s\|^2\ge\alpha_1(\|\mathbf{x}\|), \tag{19}$$

for p the minimum eigenvalue of $\mathbf{P}$, and $\alpha_1(\|\mathbf{x}\|)=a_1\cdot\|\mathbf{x}\|^2$ with a_1 given in [44], and also to

$$V\le\sum_{i=m,s}\frac{\lambda_{i2}}{2}\cdot\|\mathbf{s}_i\|^2+\frac{P}{2}\cdot\|\mathbf{q}_m-\mathbf{q}_s\|^2\le\alpha_2(\|\mathbf{x}\|), \tag{20}$$

for P the maximum eigenvalue of $\mathbf{P}$, and $\alpha_2(\|\mathbf{x}\|)=a_2\cdot\|\mathbf{x}\|^2$ with a_2 given in [44]. Because functions α_1 and α_2 are of class $\mathcal{K}_\infty$, V satisfies condition a) of Theorem T.1.

If condition (18) is satisfied, $\dot{V}$ in (16) can be further upper-bounded by:

$$\dot{V}\le-\kappa\cdot V+\frac{1}{4\omega}\cdot\|\mathbf{u}\|^2. \tag{21}$$

Then, choosing class $\mathcal{K}$ functions:

$$\alpha_3(\|\mathbf{x}\|)=\frac{a_1\kappa}{2}\cdot\|\mathbf{x}\|^2,\text{ and }\rho(\|\mathbf{u}\|)=\sqrt{\frac{1}{2a_1\kappa\omega}}\cdot\|\mathbf{u}\|, \tag{22}$$

ensures that V in (11) also satisfies condition b) of Theorem T.1 and thus, that the teleoperator is ISS. ■

Corollary 1. *ISS teleoperation by Theorem 1 renders invariant the set:*

$$\mathcal{S}_I=\left\{\mathbf{q}_m-\mathbf{q}_s:\ \|\mathbf{q}_m-\mathbf{q}_s\|^2\le\frac{2}{p}\cdot\left(V_0+\frac{\overline{\tau}^2}{4\kappa\omega}\right)\right\}, \tag{23}$$

and globally exponentially attractive the set:

$$\mathcal{S}_A=\left\{\mathbf{q}_m-\mathbf{q}_s:\ \|\mathbf{q}_m-\mathbf{q}_s\|^2\le\frac{\overline{\tau}^2}{2p\kappa\omega}\right\}, \tag{24}$$

where $\overline{\tau}^2=\overline{\tau}_h^2+\overline{\tau}_e^2$.

Proof. The proof is given in [44] and is omitted here. ■

B. ISS Teleoperation With Time-Varying Delays

For each robot, construct the following auxiliary system (proxy):

$$\begin{aligned} \hat{\mathbf{M}}_i\ddot{\hat{\mathbf{q}}}_i=&-\hat{\mathbf{K}}_i\cdot\left[\dot{\hat{\mathbf{q}}}_i+\hat{\sigma}\cdot\left(\mathbf{P}_i\cdot(\hat{\mathbf{q}}_i-\mathbf{q}_i)+\hat{\mathbf{P}}\cdot(\hat{\mathbf{q}}_i-\hat{\mathbf{q}}_{jd})\right)\right] \\ &-\hat{\mathbf{D}}_i\dot{\hat{\mathbf{q}}}_i-\mathbf{P}_i\cdot(\hat{\mathbf{q}}_i-\mathbf{q}_i)-\hat{\mathbf{P}}\cdot(\hat{\mathbf{q}}_i-\hat{\mathbf{q}}_{jd}), \end{aligned} \tag{25}$$

where: $i,j=m,s$ and $i\neq j$; $\hat{\sigma}>0$; $\hat{\mathbf{M}}_i$, $\hat{\mathbf{K}}_i$, $\hat{\mathbf{D}}_i$, $\mathbf{P}_i$ and $\hat{\mathbf{P}}$ are diagonal positive definite matrices to be determined; and $\hat{\mathbf{q}}_{jd}=\hat{\mathbf{q}}_j(t-d_j)$ is the output of the auxiliary system of robot j received with a delay d_j by robot i. Let the sliding surface of the proxy of robot i be:

$$\hat{\mathbf{s}}_i=\dot{\hat{\mathbf{q}}}_i+\hat{\sigma}\cdot\hat{\mathbf{e}}_i, \tag{26}$$

with:

$$\hat{\mathbf{e}}_i=\mathbf{P}_i\cdot(\hat{\mathbf{q}}_i-\mathbf{q}_i)+\hat{\mathbf{P}}\cdot(\hat{\mathbf{q}}_i-\hat{\mathbf{q}}_j). \tag{27}$$

Then, the auxiliary dynamics can be rearranged in the form:

$$\begin{aligned} \hat{\mathbf{M}}_i\dot{\hat{\mathbf{s}}}_i=&\hat{\sigma}\cdot\hat{\mathbf{M}}_i\left[\mathbf{P}_i\cdot\left(\dot{\hat{\mathbf{q}}}_i-\dot{\mathbf{q}}_i\right)+\hat{\mathbf{P}}\cdot\left(\dot{\hat{\mathbf{q}}}_i-\dot{\hat{\mathbf{q}}}_j\right)\right]-\hat{\mathbf{e}}_i \\ &-\hat{\mathbf{K}}_i\hat{\mathbf{s}}_i-\left(\hat{\sigma}\cdot\hat{\mathbf{K}}_i+\mathbf{I}\right)\cdot\hat{\mathbf{P}}\cdot(\hat{\mathbf{q}}_j-\hat{\mathbf{q}}_{jd})-\hat{\mathbf{D}}_i\dot{\hat{\mathbf{q}}}_i. \end{aligned} \tag{28}$$

Let the sliding surface of robot i be:

$$\mathbf{s}_i=\dot{\mathbf{q}}_i+\sigma\cdot(\mathbf{q}_i-\hat{\mathbf{q}}_i), \tag{29}$$

with $\sigma>0$. As in Section III-A, the master and slave dynamics can be transformed into (8) but with mismatch:

$$\boldsymbol{\Delta}_i=\mathbf{M}_i(\mathbf{q}_i)\cdot\left(\dot{\mathbf{q}}_i-\dot{\hat{\mathbf{q}}}_i\right)+\mathbf{C}_i(\mathbf{q}_i,\dot{\mathbf{q}}_i)\cdot(\mathbf{q}_i-\hat{\mathbf{q}}_i). \tag{30}$$

Correspondingly, the master and slave controllers are designed by:

$$\boldsymbol{\tau}_i=-\mathbf{K}_i(\dot{\mathbf{q}}_i)\cdot\mathbf{s}_i-\mathbf{P}_i\cdot(\mathbf{q}_i-\hat{\mathbf{q}}_i)-\mathbf{D}_i\dot{\mathbf{q}}_i, \tag{31}$$

with $\mathbf{K}_i(\dot{\mathbf{q}}_i)$ and $\mathbf{D}_i$ diagonal positive definite gain matrices to be determined.

Remark 3. As illustrated in Figure 2, the auxiliary systems (25) have inertia $\hat{\mathbf{M}}_i$, are connected to each other

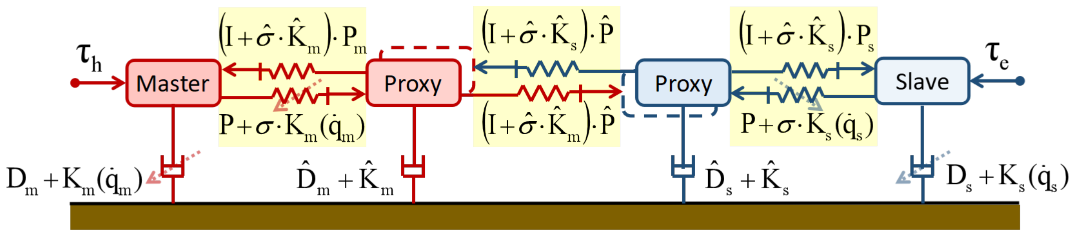

Figure 2. The teleoperator (1) in closed-loop with the control (25) and (31).

through static Proportional control, and are driven by the master and slave through static interconnection and damping control. In contrast, the master and slave are connected to their proxies by the dynamic interconnection and damping injection controls (31), which are updated according to each robot velocity $\dot{\mathbf{q}}_i$. Thus, the delays distort only information transmitted between statically coupled proxies and classical damping injection [17] can overcome their destabilizing effect. The state-dependent mismatches $\boldsymbol{\Delta}_i$ in (30) affect only the master and slave, as in the case of non-delayed communications in Section III-A. The dynamic control strategy (31) will be designed in Theorem 2 to address these mismatches.

Stability is validated using the Lyapunov candidate $V = V_1 + V_2$ with:

$$\begin{aligned} V_1 =& \frac{1}{2}\sum_{i=m,s}\left[\mathbf{s}_i^{\mathsf{T}}\mathbf{M}_i(\mathbf{q}_i)\cdot\mathbf{s}_i + (\mathbf{q}_i-\hat{\mathbf{q}}_i)^{\mathsf{T}}\mathbf{P}_i\cdot(\mathbf{q}_i-\hat{\mathbf{q}}_i)\right] \\ &+\frac{1}{2}\sum_{i=m,s}\hat{\mathbf{s}}_i^{\mathsf{T}}\hat{\mathbf{M}}_i\hat{\mathbf{s}}_i + \frac{1}{2}(\hat{\mathbf{q}}_m-\hat{\mathbf{q}}_s)^{\mathsf{T}}\hat{\mathbf{P}}\cdot(\hat{\mathbf{q}}_m-\hat{\mathbf{q}}_s), \end{aligned} \tag{32}$$

$$V_2 = \sum_{i=m,s}\int_{-\bar{d}_i}^{0}\int_{t+\theta}^{t} e^{-\gamma(t-\xi)}\cdot\dot{\mathbf{q}}_i^{\mathsf{T}}(\xi)\mathbf{Q}_i\dot{\mathbf{q}}_i(\xi)d\xi d\theta, \tag{33}$$

account for the kinetic and potential energy of the overall system, and the energy injected by time-varying delays, respectively, where $\mathbf{Q}_i \succ \mathbf{0}$, $i = m, s$.

Using property P.2, the time derivative of V_1 along the transformed master and slave dynamics (8) and their auxiliary dynamics (28) is:

$$\begin{aligned} \dot{V}_1 =& \sum_{i=m,s}\Big[\sigma\cdot\mathbf{s}_i^{\mathsf{T}}\boldsymbol{\Delta}_i - \mathbf{s}_i^{\mathsf{T}}\mathbf{K}_i(\dot{\mathbf{q}}_i)\cdot\mathbf{s}_i - \mathbf{s}_i^{\mathsf{T}}\mathbf{P}_i\cdot(\mathbf{q}_i-\hat{\mathbf{q}}_i) \\ &\qquad - \mathbf{s}_i^{\mathsf{T}}\mathbf{D}_i\dot{\mathbf{q}}_i - \hat{\mathbf{s}}_i^{\mathsf{T}}\hat{\mathbf{K}}_i\hat{\mathbf{s}}_i - \hat{\mathbf{s}}_i^{\mathsf{T}}\hat{\mathbf{e}}_i - \hat{\mathbf{s}}_i^{\mathsf{T}}\hat{\mathbf{D}}_i\dot{\hat{\mathbf{q}}}_i \\ &\qquad + \hat{\sigma}\cdot\hat{\mathbf{s}}_i^{\mathsf{T}}\hat{\mathbf{M}}_i\mathbf{P}_i\cdot\left(\dot{\hat{\mathbf{q}}}_i-\dot{\mathbf{q}}_i\right)\Big] + \mathbf{s}_m^{\mathsf{T}}\boldsymbol{\tau}_h + \mathbf{s}_s^{\mathsf{T}}\boldsymbol{\tau}_e \\ &- \sum_{i=m,s}\hat{\mathbf{s}}_i^{\mathsf{T}}\left(\hat{\sigma}\cdot\hat{\mathbf{K}}_i+\mathbf{I}\right)\cdot\hat{\mathbf{P}}\cdot(\hat{\mathbf{q}}_j-\hat{\mathbf{q}}_{jd}) \\ &+ \sum_{i=m,s}\hat{\sigma}\cdot\hat{\mathbf{s}}_i^{\mathsf{T}}\hat{\mathbf{M}}_i\hat{\mathbf{P}}\cdot\left(\dot{\hat{\mathbf{q}}}_i-\dot{\hat{\mathbf{q}}}_j\right) + \dot{\hat{\mathbf{q}}}_i^{\mathsf{T}}\hat{\mathbf{P}}\cdot(\hat{\mathbf{q}}_i-\hat{\mathbf{q}}_j) \\ &+ \sum_{i=m,s}\left[\dot{\mathbf{q}}_i^{\mathsf{T}}\mathbf{P}_i\cdot(\mathbf{q}_i-\hat{\mathbf{q}}_i) + \dot{\hat{\mathbf{q}}}_i^{\mathsf{T}}\mathbf{P}_i\cdot(\hat{\mathbf{q}}_i-\mathbf{q}_i)\right], \end{aligned} \tag{34}$$

where $j = s, m$ for $i = m, s$, respectively. The derivative of V_2 is bounded by:

$$\begin{aligned} \dot{V}_2 \leq& -\gamma\cdot V_2 + \sum_{i=m,s}\bar{d}_i\cdot\dot{\mathbf{q}}_i^{\mathsf{T}}\mathbf{Q}_i\dot{\mathbf{q}}_i \\ &- \sum_{i=m,s}e^{-\gamma\bar{d}_i}\cdot\int_{t-d_i}^{t}\dot{\mathbf{q}}_i^{\mathsf{T}}(\xi)\mathbf{Q}_i\dot{\mathbf{q}}_i(\xi)d\xi. \end{aligned} \tag{35}$$

By Property P.3, the definition of mismatches $\boldsymbol{\Delta}_i$ in (30) further leads to:

$$\begin{aligned} \mathbf{s}_i^{\mathsf{T}}\boldsymbol{\Delta}_i \leq& \lambda_{i2}\cdot\left(\mathbf{s}_i^{\mathsf{T}}\mathbf{s}_i + \frac{1}{2}\dot{\mathbf{q}}_i^{\mathsf{T}}\dot{\mathbf{q}}_i + \frac{1}{2}\dot{\hat{\mathbf{q}}}_i^{\mathsf{T}}\dot{\hat{\mathbf{q}}}_i\right) \\ &+ c_i\cdot\left(\|\dot{\mathbf{q}}_i\|^2\cdot\mathbf{s}_i^{\mathsf{T}}\mathbf{s}_i + \frac{\|\mathbf{q}_i-\hat{\mathbf{q}}_i\|^2}{4}\right). \end{aligned} \tag{36}$$

The sliding surfaces $\mathbf{s}_i$ designed in (29) imply that:

$$\begin{aligned} &\dot{\mathbf{q}}_i^{\mathsf{T}}\mathbf{P}_i\cdot(\mathbf{q}_i-\hat{\mathbf{q}}_i) - \mathbf{s}_i^{\mathsf{T}}\mathbf{P}_i\cdot(\mathbf{q}_i-\hat{\mathbf{q}}_i) - \mathbf{s}_i^{\mathsf{T}}\mathbf{D}_i\dot{\mathbf{q}}_i \\ \leq& -\sigma\cdot(\mathbf{q}_i-\hat{\mathbf{q}}_i)^{\mathsf{T}}\left(\mathbf{P}_i-\frac{\mu_i}{4}\cdot\mathbf{D}_i\right)\cdot(\mathbf{q}_i-\hat{\mathbf{q}}_i) \\ &- \left(1-\frac{\sigma}{\mu_i}\right)\cdot\dot{\mathbf{q}}_i^{\mathsf{T}}\mathbf{D}_i\dot{\mathbf{q}}_i \end{aligned} \tag{37}$$

with $\mu_i > 0$. Similarly, the sliding surfaces $\hat{\mathbf{s}}_i$ (26) imply that:

$$\begin{aligned} &\dot{\hat{\mathbf{q}}}_i^{\mathsf{T}}\mathbf{P}_i\cdot(\hat{\mathbf{q}}_i-\mathbf{q}_i) - \hat{\mathbf{s}}_i^{\mathsf{T}}\hat{\mathbf{e}}_i - \hat{\mathbf{s}}_i^{\mathsf{T}}\hat{\mathbf{D}}_i\dot{\hat{\mathbf{q}}}_i + \dot{\hat{\mathbf{q}}}_i^{\mathsf{T}}\hat{\mathbf{P}}\cdot(\hat{\mathbf{q}}_i-\hat{\mathbf{q}}_j) \\ \leq& -\left(1-\frac{\hat{\sigma}}{\nu_i}\right)\cdot\dot{\hat{\mathbf{q}}}_i^{\mathsf{T}}\hat{\mathbf{D}}_i\dot{\hat{\mathbf{q}}}_i - \hat{\sigma}\cdot\hat{\mathbf{e}}_i^{\mathsf{T}}\left(\mathbf{I}-\frac{\nu_i}{4}\cdot\hat{\mathbf{D}}_i\right)\cdot\hat{\mathbf{e}}_i \end{aligned} \tag{38}$$

with ν_i a positive constant, and that:

$$\begin{aligned} &\hat{\mathbf{s}}_i^{\mathsf{T}}\hat{\mathbf{M}}_i\hat{\mathbf{P}}\cdot\left(\dot{\hat{\mathbf{q}}}_i-\dot{\hat{\mathbf{q}}}_j\right) + \hat{\mathbf{s}}_i^{\mathsf{T}}\hat{\mathbf{M}}_i\mathbf{P}_i\cdot\left(\dot{\hat{\mathbf{q}}}_i-\dot{\mathbf{q}}_i\right) \\ \leq& \zeta_i\cdot\hat{\mathbf{s}}_i^{\mathsf{T}}\left(\hat{\mathbf{P}}\hat{\mathbf{P}}+\mathbf{P}_i\mathbf{P}_i\right)\cdot\hat{\mathbf{s}}_i + \frac{\hat{\lambda}_{i2}^2}{2\zeta_i}\cdot\left(2\dot{\hat{\mathbf{q}}}_i^{\mathsf{T}}\dot{\hat{\mathbf{q}}}_i + \dot{\hat{\mathbf{q}}}_j^{\mathsf{T}}\dot{\hat{\mathbf{q}}}_j + \dot{\mathbf{q}}_i^{\mathsf{T}}\dot{\mathbf{q}}_i\right) \end{aligned} \tag{39}$$

with ζ_i another positive constant and $\hat{\lambda}_{i2}$ the maximum eigenvalue of $\hat{\mathbf{M}}_i$. Then, Lemma 1 in [18] yields:

$$\begin{aligned} &-\hat{\mathbf{s}}_i^{\mathsf{T}}\left(\hat{\sigma}\cdot\hat{\mathbf{K}}_i+\mathbf{I}\right)\cdot\hat{\mathbf{P}}\cdot(\hat{\mathbf{q}}_j-\hat{\mathbf{q}}_{jd}) \\ &-e^{-\gamma\bar{d}_j}\cdot\int_{t-d_j}^{t}\dot{\hat{\mathbf{q}}}_j^{\mathsf{T}}(\xi)\mathbf{Q}_j\dot{\hat{\mathbf{q}}}_j(\xi)d\xi \\ \leq& \frac{\bar{d}_j}{4}\cdot e^{\gamma\bar{d}_j}\cdot\hat{\mathbf{s}}_i^{\mathsf{T}}\left(\hat{\sigma}\cdot\hat{\mathbf{K}}_i+\mathbf{I}\right)\cdot\hat{\mathbf{P}}\mathbf{Q}_j^{-1}\hat{\mathbf{P}}\left(\hat{\sigma}\cdot\hat{\mathbf{K}}_i+\mathbf{I}\right)\cdot\hat{\mathbf{s}}_i. \end{aligned} \tag{40}$$

After substitutions from (36)-(40) and (15), the sum of (34) and (35) leads to:

$$\begin{aligned}\dot{V} \leq -\sum_{i=m,s}\Big[&\mathbf{s}_i^\top\overline{\mathbf{K}}_i(\dot{\mathbf{q}}_i)\cdot\mathbf{s}_i+(\mathbf{q}_i-\hat{\mathbf{q}}_i)^\top\overline{\mathbf{P}}_i\cdot(\mathbf{q}_i-\hat{\mathbf{q}}_i)\\&+\hat{\mathbf{s}}_i^\top\tilde{\mathbf{K}}_i\hat{\mathbf{s}}_i+\hat{\sigma}\cdot\hat{\mathbf{e}}_i^\top\cdot\left(\mathbf{I}-\frac{\nu_i}{4}\cdot\hat{\mathbf{D}}_i\right)\cdot\hat{\mathbf{e}}_i+\dot{\mathbf{q}}_i^\top\overline{\mathbf{D}}_i\dot{\mathbf{q}}_i\\&+\dot{\hat{\mathbf{q}}}_i^\top\tilde{\mathbf{D}}_i\dot{\hat{\mathbf{q}}}_i\Big]-\gamma\cdot V_2+\frac{\|\boldsymbol{\tau}_h\|^2+\|\boldsymbol{\tau}_e\|^2}{4\omega},\end{aligned} \tag{41}$$

where $\chi_{ij}=\sigma\cdot\lambda_{i2}+2\hat{\sigma}\cdot\hat{\lambda}_{i2}^2/\zeta_i+\hat{\sigma}\cdot\hat{\lambda}_{j2}^2/\zeta_j$ and:

$$\begin{aligned}\overline{\mathbf{K}}_i(\dot{\mathbf{q}}_i)=&\mathbf{K}_i(\dot{\mathbf{q}}_i)-\left(\sigma\cdot\lambda_{i2}+\sigma\cdot c_i\cdot\|\dot{\mathbf{q}}_i\|^2+\omega_i\right)\cdot\mathbf{I},\\\overline{\mathbf{P}}_i=&\sigma\cdot\mathbf{P}_i-\frac{\sigma}{4}\cdot\left(c_i\cdot\mathbf{I}+\mu_i\cdot\mathbf{D}_i\right),\\\overline{\mathbf{D}}_i=&\left(1-\frac{\sigma}{\mu_i}\right)\cdot\mathbf{D}_i-\frac{1}{2}\cdot\left(\sigma\cdot\lambda_{i2}+\frac{\hat{\sigma}}{\zeta_i}\cdot\hat{\lambda}_{i2}^2\right)\cdot\mathbf{I},\\\tilde{\mathbf{K}}_i=&\hat{\mathbf{K}}_i-\hat{\sigma}\cdot\zeta_i\cdot\left(\hat{\mathbf{P}}\hat{\mathbf{P}}+\mathbf{P}_i\mathbf{P}_i\right)\\&-\frac{\overline{d}_j}{4}\cdot e^{\gamma\overline{d}_j}\cdot\left(\hat{\sigma}\cdot\hat{\mathbf{K}}_i+\mathbf{I}\right)\cdot\hat{\mathbf{P}}\mathbf{Q}_j^{-1}\hat{\mathbf{P}}\left(\hat{\sigma}\cdot\hat{\mathbf{K}}_i+\mathbf{I}\right),\\\tilde{\mathbf{D}}_i=&\left(1-\frac{\hat{\sigma}}{\nu_i}\right)\cdot\hat{\mathbf{D}}_i-\overline{d}_i\cdot\mathbf{Q}_i-\frac{\chi_{ij}}{2}\cdot\mathbf{I}.\end{aligned} \tag{42}$$

Letting $\tilde{\mathbf{q}}=\left[(\mathbf{q}_m-\hat{\mathbf{q}}_m)^\top,(\mathbf{q}_s-\hat{\mathbf{q}}_s)^\top,(\hat{\mathbf{q}}_m-\hat{\mathbf{q}}_s)^\top\right]^\top$ and using the definition of $\hat{\mathbf{e}}_i$ in (27) lead to:

$$\begin{aligned}\sum_{i=m,s}\Big[&(\mathbf{q}_i-\hat{\mathbf{q}}_i)^\top\overline{\mathbf{P}}_i(\mathbf{q}_i-\hat{\mathbf{q}}_i)\\&+\hat{\sigma}\cdot\hat{\mathbf{e}}_i^\top\cdot\left(\mathbf{I}-\frac{\nu_i}{4}\cdot\hat{\mathbf{D}}_i\right)\cdot\hat{\mathbf{e}}_i\Big]=\tilde{\mathbf{q}}^\top\tilde{\mathbf{P}}\tilde{\mathbf{q}},\end{aligned} \tag{43}$$

where $\tilde{\mathbf{P}}=[\mathbf{B}_{rc}]$ with $\mathbf{B}_{12}=\mathbf{B}_{21}=\mathbf{0}$ and:

$$\begin{aligned}\mathbf{B}_{11}=&\mathbf{P}_m\left(\mathbf{I}-\frac{\nu_m}{4}\cdot\hat{\mathbf{D}}_m\right)\cdot\mathbf{P}_m+\overline{\mathbf{P}}_m,\\\mathbf{B}_{13}=&\mathbf{B}_{31}^\top=\mathbf{P}_m\left(\mathbf{I}-\frac{\nu_m}{4}\cdot\hat{\mathbf{D}}_m\right)\cdot\hat{\mathbf{P}},\\\mathbf{B}_{22}=&\mathbf{P}_s\left(\mathbf{I}-\frac{\nu_s}{4}\cdot\hat{\mathbf{D}}_s\right)\cdot\mathbf{P}_s+\overline{\mathbf{P}}_s,\\\mathbf{B}_{23}=&\mathbf{B}_{32}^\top=\mathbf{P}_s\left(\mathbf{I}-\frac{\nu_s}{4}\cdot\hat{\mathbf{D}}_s\right)\cdot\hat{\mathbf{P}},\\\mathbf{B}_{33}=&\hat{\mathbf{P}}\left(2\mathbf{I}-\frac{\nu_m}{4}\cdot\hat{\mathbf{D}}_m-\frac{\nu_s}{4}\cdot\hat{\mathbf{D}}_s\right)\hat{\mathbf{P}}.\end{aligned} \tag{44}$$

The following proposition about $\tilde{\mathbf{P}}$ contributes to proving ISS teleoperation in Theorem 2.

Proposition 1. *Let:*

$$\mathbf{P}_i=\mathbf{P},\quad\hat{\mathbf{D}}_i=\hat{\mathbf{D}},\quad\textit{and}\quad\nu_i=\nu, \tag{45}$$

$$\textit{and}\quad\overline{\mathbf{P}}_i\succ\mathbf{0},\quad\mathbf{I}-\frac{\nu}{4}\cdot\hat{\mathbf{D}}\succ\mathbf{0}, \tag{46}$$

for $i=m,s$. Then there exists $\delta>0$ such that:

$$\tilde{\mathbf{P}}\succeq\frac{\delta}{2}\cdot\max\left(\mathbf{P},\hat{\mathbf{P}}\right). \tag{47}$$

Proof. The proof is given in [44] and is omitted here. ■

Theorem 2. *The teleoperator* (1) *in closed-loop with* (25) *and* (31) *is ISS with input $\mathbf{u}=[\boldsymbol{\tau}_h^\top\ \boldsymbol{\tau}_e^\top]^\top$ and state $\mathbf{x}=[\dot{\mathbf{q}}_m^\top\ \dot{\mathbf{q}}_s^\top\ \dot{\hat{\mathbf{q}}}_m^\top\ \dot{\hat{\mathbf{q}}}_s^\top\ (\mathbf{q}_m-\hat{\mathbf{q}}_m)^\top\ (\mathbf{q}_s-\hat{\mathbf{q}}_s)^\top\ (\hat{\mathbf{q}}_m-\hat{\mathbf{q}}_s)^\top]^\top$ if the parameters and control gains satisfy conditions* (45)-(46) *and:*

$$\overline{\mathbf{K}}_i(\dot{\mathbf{q}}_i)\succeq\frac{\psi}{2}\cdot\lambda_{i2}\cdot\mathbf{I},\quad\tilde{\mathbf{K}}_i\succeq\frac{\psi}{2}\cdot\hat{\lambda}_{i2}\cdot\mathbf{I},\quad\overline{\mathbf{D}}_i\succeq\mathbf{0},\quad\tilde{\mathbf{D}}_i\succeq\mathbf{0}, \tag{48}$$

where $i=m,s$ and $\psi>0$.

Proof. Let $p\cdot\mathbf{I}\preceq\mathbf{P}\preceq P\cdot\mathbf{I}$ and $\hat{p}\cdot\mathbf{I}\preceq\hat{\mathbf{P}}\preceq\hat{P}\cdot\mathbf{I}$. The Lyapunov candidate V can be lower-bounded by:

$$\begin{aligned}V\geq&\frac{1}{2}\sum_{i=m,s}\left(\lambda_{i1}\cdot\|\mathbf{s}_i\|^2+\hat{\lambda}_{i1}\cdot\|\hat{\mathbf{s}}_i\|^2+p\cdot\|\mathbf{q}_i-\hat{\mathbf{q}}_i\|^2\right)\\&+\frac{\hat{p}}{2}\cdot\|\hat{\mathbf{q}}_m-\hat{\mathbf{q}}_s\|^2\geq\hat{\alpha}_3(\|\mathbf{x}\|),\end{aligned} \tag{49}$$

where $\hat{\lambda}_{i1}$ is the minimum eigenvalue of $\hat{\mathbf{M}}_i$, and $\hat{\alpha}_3(\|\mathbf{x}\|)=a_3\cdot\|\mathbf{x}\|^2$ is a function of class $\mathcal{K}_\infty$ with a_3 given in [44]. Further, the definition of V_2 indicates that:

$$V_2\leq\sum_{i=m,s}\frac{1}{2}\cdot\overline{d}_i^2\overline{Q}_i\cdot|\dot{\mathbf{q}}_i|_r^2, \tag{50}$$

where $\overline{Q}_i$ is the maximum eigenvalue of $\mathbf{Q}_i$. Then V can be upper-bounded by:

$$\begin{aligned}V\leq&\frac{1}{2}\sum_{i=m,s}\left(\lambda_{i2}\cdot\|\mathbf{s}_i\|^2+\hat{\lambda}_{i2}\cdot\|\hat{\mathbf{s}}_i\|^2+P\cdot\|\mathbf{q}_i-\hat{\mathbf{q}}_i\|^2\right)\\&+\frac{\hat{P}}{2}\cdot\|\hat{\mathbf{q}}_m-\hat{\mathbf{q}}_s\|^2+V_2\leq\hat{\alpha}_4(|\mathbf{x}|_r),\end{aligned} \tag{51}$$

where $\hat{\alpha}_4(|\mathbf{x}|_r)=a_4\cdot|\mathbf{x}|_r^2$ with a_4 given in [44]. Let $\gamma_a=\sqrt{a_3}$ and $\overline{\gamma}_a=\sqrt{a_4}$, define $|\mathbf{x}_t|_a=\sqrt{V(\mathbf{x}_t)}$ to satisfy (2), and select functions $\alpha_1(\|\mathbf{x}\|)=\hat{\alpha}_3(\|\mathbf{x}\|)$ and $\alpha_2(|\mathbf{x}_t|_a)=|\mathbf{x}_t|_a^2$ of class $\mathcal{K}_\infty$ to trivially guarantee condition a) of Theorem T.2.

After substitution from (43) in (41), using condition (48) and setting $\kappa=\min(\psi,\delta,\gamma)$, $\dot{V}$ can be upper-bounded by:

$$\dot{V}\leq-\kappa\cdot V+\frac{1}{4\omega}\cdot\|\mathbf{u}\|^2. \tag{52}$$

Then the functions α_3 and ρ of class $\mathcal{K}$ and defined by:

$$\alpha_3(|\mathbf{x}_t|_a)=\frac{\kappa}{2}\cdot|\mathbf{x}_t|_a^2,\text{ and }\rho(\|\mathbf{u}\|)=\sqrt{\frac{1}{2\kappa\omega}}\cdot\|\mathbf{u}\| \tag{53}$$

ensure condition b) of Theorem T.2 [43].

Thus, the Lyapunov candidate V obeys both conditions of Theorem T.2 [43] and the teleoperator is ISS. ■

Corollary 2. *ISS teleoperation by Theorem 2 renders invariant the set:*

$$\mathcal{S}_I=\left\{\mathbf{q}_m-\mathbf{q}_s:\ \|\mathbf{q}_m-\mathbf{q}_s\|^2\leq\frac{4}{p'}\cdot\left(V_0+\frac{\overline{\tau}^2}{4\kappa\omega}\right)\right\}, \tag{54}$$

and globally attractive the set:

$$\mathcal{S}_A=\left\{\mathbf{q}_m-\mathbf{q}_s:\ \|\mathbf{q}_m-\mathbf{q}_s\|^2\leq\frac{\overline{\tau}^2}{p'\kappa\omega}\right\}, \tag{55}$$

where $p'=\min(p_m,p_s,\hat{p})$.

Proof. The proof is given in [44] and is omitted here. ■

C. Discussion

Closed-loop bilateral teleoperation includes uncertain and practically uncontrollable user and environment dynamics. To robustly stabilize closed-loop teleoperation, this paper regards the user and environment forces as time-varying and unpredictable teleoperator inputs, and designs controllers to render the teleoperator input-to-state stable. ISS teleoperation guarantees robust position synchronization of the master and slave under user and environment perturbations [45], and thus, reflects slave-environment interactions to the operator [30]. According to the definitions in Section II-B, ISS teleoperation implies: (i) $\{\dot{\mathbf{q}}_m, \dot{\mathbf{q}}_s, \mathbf{q}_m - \mathbf{q}_s\} \in \mathcal{L}_\infty$; and (ii) $\{\dot{\mathbf{q}}_m, \dot{\mathbf{q}}_s, \mathbf{q}_m - \mathbf{q}_s\} \to \mathbf{0}$ if $\boldsymbol{\tau}_h = \boldsymbol{\tau}_e = \mathbf{0}$. Thus, ISS teleoperation matches the stability definition in [29] for bilateral teleoperation.

According to Corollary 1 and Corollary 2, an invariant set $\mathcal{S}_I$ and a globally attractive set $\mathcal{S}_A$ characterize the master-slave position error $\mathbf{q}_m(t) - \mathbf{q}_s(t)$ of ISS teleoperation: the error stays in $\mathcal{S}_I$ and exponentially approaches $\mathcal{S}_A$ for $t \geq 0$. The Lebesgue measure of $\mathcal{S}_I$ and $\mathcal{S}_A$ can be reduced by increasing p_i, $\hat{p}$, ω and κ. The speed of (exponential) convergence to $\mathcal{S}_A$ is determined by κ. When the user and environment forces disappear, the steady-state position error becomes zero by the definition of input-to-state stability.

The controllers (10) and (31) assume gravity-compensated master and slave. Inaccurate gravity compensation can introduce bounded disturbances $\boldsymbol{\delta}_i$, $i = m, s$, in practical teleoperation systems. By including $\boldsymbol{\delta}_i$ in the teleoperator input $\mathbf{u}^\star = [(\boldsymbol{\tau}_h + \boldsymbol{\delta}_m)^\mathsf{T}\ (\boldsymbol{\tau}_e + \boldsymbol{\delta}_s)^\mathsf{T}]^\mathsf{T}$, the proposed dynamic strategy can render the teleoperator ISS with the augmented input $\mathbf{u}^\star$ and the same state $\mathbf{x}$ as defined in Theorem 1 and Theorem 2. Alternatively, minor modifications of adaptive control techniques [22] can be employed in the design to provide parameter estimates and to facilitate position synchronization.

IV. Experiments

In this section, experiments with a pair of Geomagic Touch haptic devices compare the dynamic interconnection and damping injection strategy to three position-based approaches: the Proportional plus damping (P+d) [17], two-layer [8] and passive set-position modulation (PSPM) [29] strategies. All controllers are designed in joint space to drive the three actuated joints indicated in Figure 3. The user seeks to drive the master along the same Cartesian path in each successive experiment. The time-varying communication delays obey $d_i \leq 5$ ms, $i = m, s$. The robust position tracking performance of the teleoperator with the four controllers is illustrated by plotting the Cartesian paths of the master and slave end-effectors, and is quantitatively evaluated through their maximum and average position errors. The video of the experiments is available at https://youtu.be/xBXDh5BX3uY.

All parameters are selected heuristically for optimal performance of each controller. All controllers connect the master and slave by Proportional control and stabilize the teleoperation by local damping injection. The robot joint positions are measured by encoders, and their joint velocities are estimated by second-order low-pass filters with recommended cut-off frequency 200 rad/s and damping ratio 1. Damping injection for all four controllers is then restricted by unreliable velocity estimation in experiments. In turn, limited damping injection constrains the Proportional gain of each controller by their design criteria. Because larger Proportional gains generally decrease position errors, the parameters of all controllers are tuned to maximize their Proportional gain for the damping gain that practically stabilizes the system. Practically, the master-slave coupling of each controller is maximally tightened without destabilizing the teleoperation experiments.

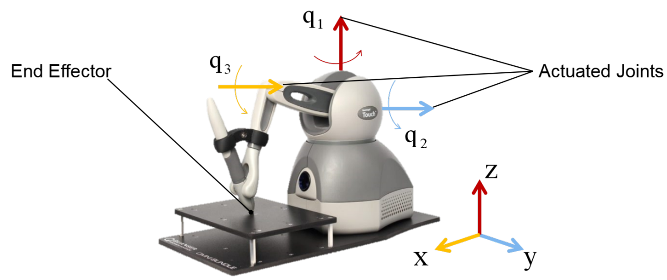

Figure 3. The Geomagic Touch haptic device with three actuated joints.

Proportional plus damping (P+d) control [17]

After selecting the damping gain $B_i = 0.01$, a maximum Proportional gain $K_i = 3.5$ can couple the master and slave stably. Figure 4 depicts the task-space paths of the master and slave end-effectors. It shows that the slave follows the master with increasing tracking error and vibration during changes of the direction of motion.

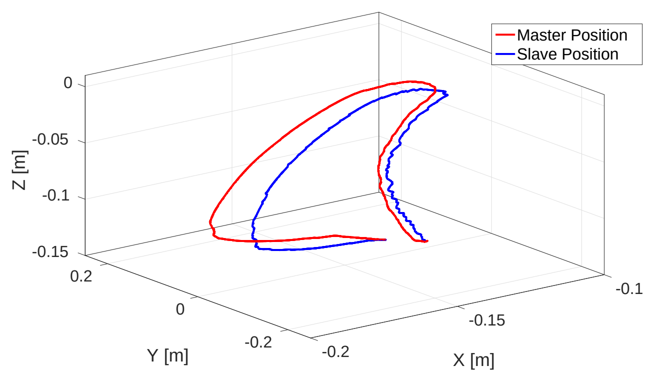

Figure 4. Task-space paths of the master and slave end-effectors under P+d control [17].

Two-layer approach [8]

After selecting master and slave energy tanks with threshold $H_D = 0.3$ J, and $\beta = 0.01$ to synchronize them quickly, a proportional gain $K_i = 3$ in the transparency layer and a nonlinear master damper with $\alpha = 0.3$ in the passivity layer maximally stiffen the master-slave coupling without destabilizing the teleoperation. The experimental end-effector paths in Figure 5 indicate position tracking similar to P+d control. Yet, momentarily active behaviours [8] lead to more severe vibrations in the final phase of this experiment.

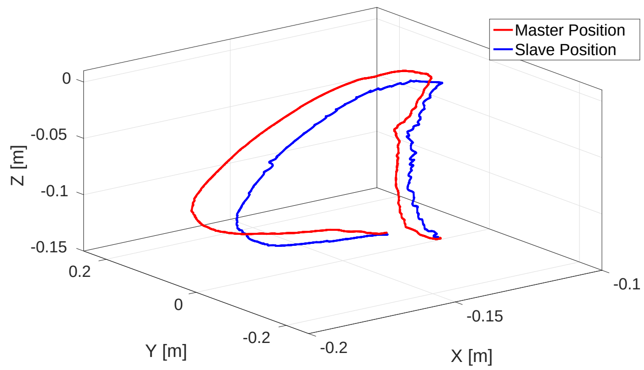

Figure 5. Task-space paths of the master and slave end-effectors under two-layer control [8].

Passive set-position modulation (PSPM) framework [29]

For an energy tank with capacity $\overline{E}_i = 0.3$ J and initial stored energy $E_i(0) = 0.15$ J, coupling and damping gains $K_i = 5$ and $B_i = 0.1$ guarantee agile and oscillation-free position tracking. The experimental results in Figure 6 show that the set-position of each robot is exactly the position of the other robot. Effectively, the controller does not modulate the reference signal of either robot, but is a static P+d controller during the experiment. Nevertheless, its triggering mechanism with a time period 0.01 s permits larger K_i and B_i gains than P+d control and, hence, couples the master and slave tighter.

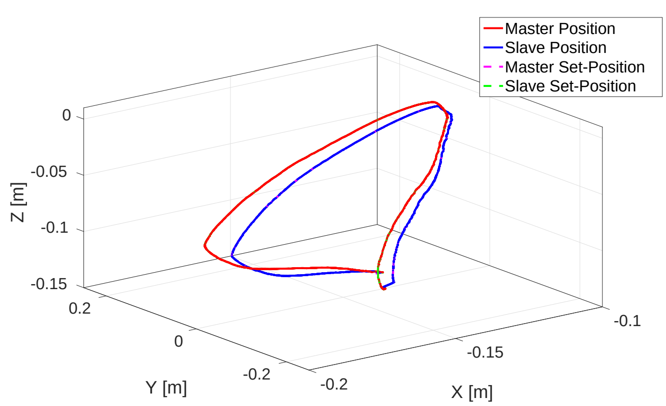

Figure 6. Task-space paths of the master and slave end-effectors under PSPM control [29].

Dynamic interconnection and damping injection

From the Euler-Lagrange model of the haptic device in [46], $\lambda_{i2} = 1.6$ and $c_i = 0.1$ can be employed in the design. After choosing $\sigma = 0.01$, $\hat{\sigma} = 0.001$, $\mu_i = 10$ and $\zeta_i = 0.1$, each robot can be connected to its proxy tightly and damped suitably while guaranteeing $\overline{\mathbf{P}}_i \succ \mathbf{0}$ and $\overline{\mathbf{D}}_i \succeq \mathbf{0}$ by setting $\mathbf{D}_i = 0.08\mathbf{I}$ and $\mathbf{P}_i = 20\mathbf{I}$. After letting $\nu_i = 0.25$, $\psi = 0.001$, $\gamma = 0.1$, $\hat{\mathbf{M}}_i = 0.01\mathbf{I}$ and $\mathbf{Q}_i = 50\mathbf{I}$, the selections $\hat{\mathbf{P}}_i = 50\mathbf{I}$, $\hat{\mathbf{D}}_i = 0.275\mathbf{I}$ and $\hat{\mathbf{K}}_i = 0.01\mathbf{I}$ make $\tilde{\mathbf{K}}_i \succeq \frac{\psi}{2} \cdot \hat{\lambda}_{i2} \cdot \mathbf{I}$ and $\tilde{\mathbf{D}}_i \succeq \mathbf{0}$ and connect the master and slave proxies tightly. With $\omega_i = 0.01$, $\mathbf{K}_i(\dot{\mathbf{q}}_i)$ can be updated according to (42) and (48) to stabilize the teleoperator. Figure 7, which plots the experimental paths of the master and slave end-effectors and of their proxies, indicates that: (a) compared to the P+d (Figure 4) and two-layer (Figure 6) control, dynamic interconnection and damping injection control eliminates vibrations when the master slows down; and (b) compared to PSPM control (Figure 5), it synchronizes the master and slave better, through larger static proportional gains $\mathbf{P}_i$, $\hat{\mathbf{P}}_i$ and $\hat{\mathbf{K}}_i$ and dynamically updated gains $\mathbf{K}_i(\dot{\mathbf{q}}_i)$.

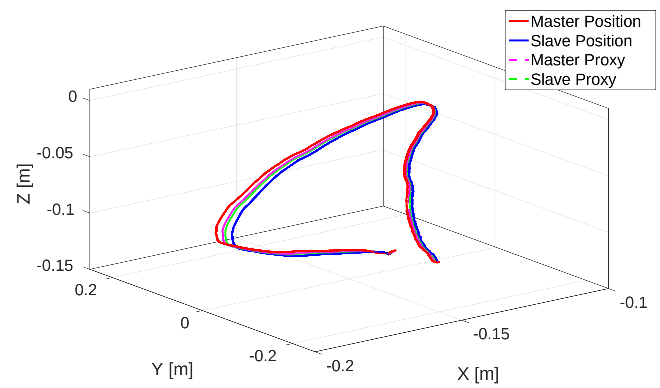

Figure 7. Task-space paths of the master and slave end-effectors under dynamic interconnection and damping injection control (25) and (31).

Table I evaluates the robust position tracking performance of the delayed teleoperator under the four controllers through the maximum tracking error:

$$\Xi_{\max} = \max_{k=1,\cdots,N} \|\text{Pos}_m(k) - \text{Pos}_s(k)\|,$$

and the average tracking error:

$$\Xi_{\text{ave}} = \frac{1}{N}\sum_{k=1}^{N} \|\text{Pos}_m(k) - \text{Pos}_s(k)\|,$$

where $\text{Pos}_i(k)$ is the position of the end effector of robot i at the k-th sampling instant, and N is the number of sampling instants. It illustrates that dynamic interconnection and damping injection can reduce both the maximum and the average master-slave position errors of bilateral teleoperation with time-varying delays. By Corollary 2, the master-slave position error can be reduced by increasing the Proportional gains. Then, a greater amount of physical damping injection is needed to practically stabilize the system. However, unreliable velocity estimations limit the amount of injected damping and hence the stiffness of the master-slave coupling by Theorem 2. Therefore, the average master-slave position error retains 1.8 mm even though the parameters of our proposed controller have been carefully tuned in the experiment.

The dynamic interconnection and damping injection controller has force feedback performance similar to the PSPM controller, and has average and maximum master feedback forces approximately 40% larger than the P+d and two-layer controllers. The larger forces are due to the larger damping injection, needed to stabilize the stiffer master-slave interconnection. To save space, the detailed force tracking is presented only in the video of the experiments available at https://youtu.be/xBXDh5BX3uY.

Table I
POSITION TRACKING ERRORS DURING TIME-DELAY TELEOPERATION UNDER FOUR CONTROLLERS.

Controller	Maximum Position Error $\Xi_{\max}$	Average Position Error Ξ_{ave}
Proportional plus damping control	25.4 mm	3.3 mm
Position-based two-layer approach	30.1 mm	3.6 mm
Passive set-position modulation framework	18.5 mm	2.6 mm
Dynamic interconnection and damping injection	10.8 mm	1.8 mm

V. CONCLUSION

This paper has presented a constructive dynamic interconnection and damping injection strategy for robust stabilization of bilateral teleoperation without, and with, time-varying delays. Lyapunov stability analysis has proven that the proposed strategy renders bilateral teleoperation exponentially input-to-state stable, even in the presence of time-varying delays. It has also shown that an invariant set and a globally attractive set characterize the master-slave position errors during teleoperation under the control of the proposed strategy. Suitable selection and updating of the control gains can decrease the master-slave position error to any prescribed level with a certain rate of convergence and, thus, can improve robust position tracking performance. Experiments have illustrated that, compared to state-of-the-art controllers, the dynamic interconnection and damping injection strategy in this paper can reduce both the maximum and the average position tracking errors during teleoperation with time-varying delays.

Practical teleoperation systems suffer from inaccurate gravity compensation and unreliable velocity measurements. Disturbances caused by inaccurate gravity compensation can increase position tracking errors. Unreliable velocity measurements impede damping injection and the modulation of control gains and thus, can destabilize the teleoperation. Future work will focus on input-to-state stability of bilateral teleoperators without gravity compensation and velocity measurements.

REFERENCES

[1] Y.-C. Liu and N. Chopra, "Control of semi-autonomous teleoperation system with time delays," *Automatica*, vol. 49, no. 6, pp. 1553–1565, 2013.

[2] S. Hirche and M. Buss, "Human-oriented control for haptic teleoperation," *Proc. IEEE*, 2012.

[3] E. J. RodrÍguez-Seda, D. Lee, and M. W. Spong, "Experimental comparison study of control architectures for bilateral teleoperators," *IEEE Transactions on Robotics*, vol. 25, no. 6, pp. 1304–1318, 2009.

[4] H. Ito, P. Pepe, and Z.-P. Jiang, "A small-gain condition for iiss of interconnected retarded systems based on lyapunov–krasovskii functionals," *Automatica*, vol. 46, no. 10, pp. 1646–1656, 2010.

[5] C. Secchi, S. Stramigioli, and C. Fantuzzi, *Control of interactive robotic interfaces: A port-Hamiltonian approach*, vol. 29. Springer Science & Business Media, 2007.

[6] P. F. Hokayem and M. W. Spong, "Bilateral teleoperation: An historical survey," *Automatica*, vol. 42, no. 12, pp. 2035 – 2057, 2006.

[7] E. Nuño, L. Basañez, and R. Ortega, "Passivity-based control for bilateral teleoperation: A tutorial," *Automatica*, vol. 47, no. 3, pp. 485 – 495, 2011.

[8] M. Franken, S. Stramigioli, S. Misra, C. Secchi, and A. Macchelli, "Bilateral telemanipulation with time delays: A two-layer approach combining passivity and transparency," *IEEE Transactions on Robotics*, vol. 27, no. 4, pp. 741–756, 2011.

[9] L. Bate, C. D. Cook, and Z. Li, "Reducing wave-based teleoperator reflections for unknown environments," *IEEE Transactions on Industrial Electronics*, vol. 58, no. 2, pp. 392–397, 2011.

[10] Y. Ye and P. X. Liu, "Improving trajectory tracking in wave-variable-based teleoperation," *IEEE/ASME Transactions on Mechatronics*, vol. 15, no. 2, pp. 321–326, Apr. 2010.

[11] D. Sun, Q. Liao, and H. Ren, "Type-2 fuzzy modeling and control for bilateral teleoperation system with dynamic uncertainties and time-varying delays," *IEEE Transactions on Industrial Electronics*, vol. 65, DOI 110.1109/TIE.2017.2719604, no. 1, pp. 447–459, 2018.

[12] N. A. Tanner and G. Niemeyer, "High-frequency acceleration feedback in wave variable telerobotics," *IEEE/ASME Transactions on Mechatronics*, vol. 11, no. 2, pp. 119–127, 2006.

[13] B. Yalcin and K. Ohnishi, "Stable and transparent time-delayed teleoperation by direct acceleration waves," *IEEE Transactions on Industrial Electronics*, vol. 57, no. 9, pp. 3228–3238, 2010.

[14] J. Rebelo and A. Schiele, "Time domain passivity controller for 4-channel time-delay bilateral teleoperation," *IEEE Transactions on Haptics*, vol. 8, no. 1, pp. 79–89, Jan. 2015.

[15] D. Sun, F. Naghdy, and H. Du, "Wave-variable-based passivity control of four-channel nonlinear bilateral teleoperation system under time delays," *IEEE/ASME Transactions on Mechatronics*, vol. 21, no. 1, pp. 238–253, 2015.

[16] D. Lee and M. W. Spong, "Passive bilateral teleoperation with constant time delay," *IEEE Transactions on Robotics*, vol. 22, no. 2, pp. 269–281, Apr. 2006.

[17] E. Nuño, R. Ortega, N. Barabanov, and L. Basañez, "A globally stable PD controller for bilateral teleoperators," *IEEE Transactions on Robotics*, vol. 24, no. 3, pp. 753–758, Jun. 2008.

[18] C. Hua and X. P. Liu, "Delay-dependent stability criteria of teleoperation systems with asymmetric time-varying delays," *IEEE Transactions on Robotics*, vol. 26, no. 5, pp. 925–932, Oct. 2010.

[19] C. Hua, Y. Yang, and X. P. Liu, "Output-feedback adaptive control of networked teleoperation system with time-varying delay and bounded inputs," *IEEE/ASME Transactions on Mechatronics*, vol. 20, no. 5, pp. 2009–2020, Oct. 2015.

[20] F. Hashemzadeh, I. Hassanzadeh, and M. Tavakoli, "Teleoperation in the presence of varying time delays and sandwich linearity in actuators," *Automatica*, vol. 49, no. 9, pp. 2813 – 2821, 2013.

[21] N. Chopra, M. W. Spong, and R. Lozano, "Synchronization of bilateral teleoperators with time delay," *Automatica*, vol. 44, no. 8, pp. 2142–2148, 2008.

[22] E. Nuño, R. Ortega, and L. Basañez, "An adaptive controller for nonlinear teleoperators," *Automatica*, vol. 46, no. 1, pp. 155–159, 2010.

[23] Y.-C. Liu and N. Chopra, "Control of semi-autonomous teleoperation system with time delays," *Automatica*, vol. 49, no. 6, pp. 1553–1565, 2013.

[24] Y. C. Liu and M. H. Khong, "Adaptive control for nonlinear teleoperators with uncertain kinematics and dynamics," *IEEE/ASME Transactions on Mechatronics*, vol. 20, no. 5, pp. 2550–2562, Oct. 2015.

[25] J.-H. Ryu, D.-S. Kwon, and B. Hannaford, "Stable teleoperation with time-domain passivity control," *IEEE Transactions on Robotics and Automation*, vol. 20, no. 2, pp. 365–373, Apr. 2004.

[26] Y. Ye, Y. J. Pan, and T. Hilliard, "Bilateral teleoperation with time-varying delay: A communication channel passification approach," *IEEE/ASME Transactions on Mechatronics*, vol. 18, no. 4, pp. 1431–1434, Aug. 2013.

[27] V. Chawda and M. K. O'Malley, "Position synchronization in bilateral teleoperation under time-varying communication delays," *IEEE/ASME Transactions on Mechatronics*, vol. 20, no. 1, pp. 245–253, 2015.

[28] J.-P. Kim and J. Ryu, "Robustly stable haptic interaction control using

an energy-bounding algorithm," *The International Journal of Robotics Research*, vol. 29, no. 6, pp. 666–679, 2010.
[29] D. Lee and K. Huang, "Passive-set-position-modulation framework for interactive robotic systems," *IEEE Transactions on Robotics*, vol. 26, no. 2, pp. 354–369, 2010.
[30] D. Heck, A. Saccon, R. Beerens, and H. Nijmeijer, "Direct force-reflecting two-layer approach for passive bilateral teleoperation with time delays," *IEEE Transactions on Robotics*, vol. 34, no. 1, pp. 194–206, 2018.
[31] K. Gu, J. Chen, and V. L. Kharitonov, *Stability of time-delay systems*. Springer Science & Business Media, 2003.
[32] A. Jafari, M. Nabeel, and J. Ryu, "The input-to-state stable (iss) approach for stabilizing haptic interaction with virtual environments," *IEEE Transactions on Robotics*, vol. 33, no. 4, pp. 948–963, Aug. 2017.
[33] S. Islam, P. X. Liu, A. El Saddik, R. Ashour, J. Dias, and L. D. Seneviratne, "Aritificial and virtual impedance interaction force reflection-based bilateral shared control for miniature unmanned aerial vehicle," *IEEE Transactions on Industrial Electronics*, vol. 66, no. 1, pp. 329–337, 2019.
[34] D. A. Lawrence, "Stability and transparency in bilateral teleoperation," *IEEE Transactions on Robotics and Automation*, vol. 9, no. 5, pp. 624–637, Oct. 1993.
[35] K. Hashtrudi-Zaad and S. E. Salcudean, "Bilateral parallel force/position teleoperation control," *Journal of Robotic Systems*, vol. 19, no. 4, pp. 155–167, 2002.
[36] T. Nozaki, T. Mizoguchi, and K. Ohnishi, "Decoupling strategy for position and force control based on modal space disturbance observer," *IEEE Transactions on Industrial Electronics*, vol. 61, no. 2, pp. 1022–1032, 2014.
[37] Y. Yokokura, K. Ohishi, and S. Katsura, "Fine force reproduction based on motion-copying system using acceleration observer," *IEEE Transactions on Industrial Electronics*, vol. 61, no. 11, pp. 6213 – 6221, 2014.
[38] R. Antonello, K. Ito, and R. Oboe, "Acceleration measurement drift rejection in motion control systems by augmented-state kinematic kalman filter," *IEEE Transactions on Industrial Electronics*, vol. 63, no. 3, pp. 1953–1961, 2016.
[39] Y. Nagatsu and S. Katsura, "Decoupling and performance enhancement of hybrid control for motion-copying sytem," *IEEE Transactions on Industrial Electronics*, vol. 64, no. 1, pp. 420–431, 2017.
[40] R. Sepulchre, M. Jankovic, and P. V. Kokotovic, *Constructive nonlinear control*. Springer Science & Business Media, 2012.
[41] M. Franken, S. Misra, and S. Stramigioli, "Stability of position-based bilateral telemanipulation systems by damping injection," in *Robotics and Automation (ICRA), 2012 IEEE International Conference on*, pp. 4300–4306. IEEE, 2012.
[42] E. D. Sontag, "Input to state stability: Basic concepts and results," in *Nonlinear and optimal control theory*, pp. 163–220. Springer, 2008.
[43] P. Pepe and Z.-P. Jiang, "A lyapunov–krasovskii methodology for ISS and iISS of time-delay systems," *Systems & Control Letters*, vol. 55, no. 12, pp. 1006–1014, 2006.
[44] Y. Yang, D. Constantinescu, and Y. Shi, "Dynamic interconnection and damping injection for input-to-state stable bilateral teleoperation," 2019, arXiv:1902.05500.
[45] I. Karafyllis, P. Pepe, and Z.-P. Jiang, "Input-to-output stability for systems described by retarded functional differential equations," *European Journal of Control*, vol. 14, no. 6, pp. 539–555, 2008.
[46] A. Nygaard, "High-level control system for remote controlled surgical robots: Haptic guidance of surgical robot," Master's thesis, Norwegian University of Science and Technology, 2008.

Yuan Yang received the B.Eng. degree in Mechanical design, manufacturing and automation from Harbin Institute of Technology, Harbin, China, in 2015, and the M.A.Sc. degree in mechanical engineering from the University of Victoria, Victoria, BC, Canada, in 2017, where he is currently persuring his PhD. degree in mechanical engineering. His current research interests include distributed control of networked dynamical systems, human robot collaboration, and safety for physical human-robot interaction.

Daniela Constantinescu received the Ph.D. degree in electrical and computer engineering from University of British Columbia, Vancouver, BC, Canada in 2005. She has been with the University of Victoria since 2005, where she is currently Associate Professor with the Department of Mechanical Engineering. Her current research interests include teleoperation and haptic systems, distributed control for network robotic systems, human robot interaction, robotics and dynamics.

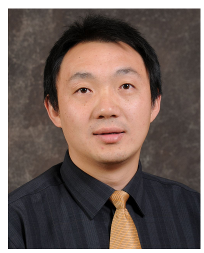

Yang Shi (SM'09-F'17) received the Ph.D. degree in electrical and computer engineering from the University of Alberta, Edmonton, AB, Canada, in 2005. From 2005 to 2009, he was a faculty member with the Department of Mechanical Engineering, University of Saskatchewan, Saskatoon, SK, Canada. He is currently a Professor with the Department of Mechanical Engineering, University of Victoria, Victoria, BC, Canada. His current research interests include networked and distributed systems, model predictive control, industrial cyber-physical systems, mechatronics and robotics, and energy systems.

Prof. Shi received the University of Saskachewan Student Union Teaching Excellence Award in 2007 and the Faculty of Engineering Teaching Excellence Award from the University of Victoria in 2012. He received the JSPS Invitation Fellowship (short-term) in 2013 and the 2015 Craigdarroch Silver Medal for Excellence in Research from the University of Victoria. He currently serves as Co-Editor-in-Chief of IEEE Transactions on Industrial Electronics, and Associate Editor for Automatica, the IEEE Transactions on Control Systems Technology, IEEE/ASME Transactions on Mechatronics, and IEEE Transactions on Cybernetics. He is the Chair of IEEE Industrial Electronics Society Technical Committee on Industrial Cyber-Physical Systems. He is a fellow of the Canadian Society for Mechanical Engineering, a Fellow of the American Society of Mechanical Engineers, Engineering Institute of Canada, and a Registered Professional Engineer in the Province of British Columbia, Canada.